Proceedings of the 2004 IEEE
International Symposium on Intelligent Control
Taipei, Taiwan, September 2-4, 2004

Robust Fuzzy Gain Scheduled visual-servoing with Sampling Time Uncertainties

Bourhane Kadmiry[†] and **Pontus Bergsten**

Abstract— **This paper addresses the robust fuzzy control problem for discrete-time nonlinear systems in the presence of sampling time uncertainties in a visual-servoing control scheme. The Takagi-Sugeno (T-S) fuzzy model is adopted for the nonlinear geometric model of a pin-hole camera, which presents second-order nonlinearities. The case of the discrete T–S fuzzy system with sampling-time uncertainty is considered and a multi-objective robust fuzzy controller design is proposed for the uncertain fuzzy system. The sufficient conditions are formulated in the form of linear matrix inequalities (LMI). The effectiveness of the proposed controller design methodology is demonstrated through numerical simulation, then tested on a EVI-D31 SONY camera.**

Keywords- Visual-servoing, T-S fuzzy gain scheduled control, Linear Matrix Inequalities, sampling time uncertainty, Lyapunov robust stability, LQR guaranteed cost, multi-objective robustness.

I. Introduction

The overall objective of the Wallenberg Laboratory for Information Technology and Autonomous Systems (WITAS) at Linköping University is the development of an intelligent command and control system, containing active-vision sensors, which supports the operation of a unmanned air vehicle (UAV). One of the UAV platforms of choice is the R50 unmanned helicopter, by Yamaha. The intended operational environment is over widely varying geographical terrain with traffic networks and vehicle interaction of variable complexity, speed, and density. The present version of the UAV platform is augmented with a camera system and robust performance for the visual-servoing scheme is desired. Robustness in this case is twofold: 1) w.r.t time delays introduced by the image processing system, these can vary in the interval $[40, 100]$ msec.; 2) w.r.t parameter uncertainties as the camera focal distance and un-modelled dynamics which reflect on the feature position in the image $[p_x, p_y]^T$ and the camera pose $[\omega_x, \omega_y]^T$. In this context, our goal is to explore the possibilities for achieving robust performance w.r.t image feature tracking, and test a control solution in both simulation and on a real camera platform. Then we implement and test the resulting controller on the camera platform –to be later on mounted on the UAV.

In this work we address the design of a controller that achieves stable and robust image feature regulation/tracking for a pan/tilt camera. The controller is obtained using a realistic nonlinear model of a pin-hole camera. The model used is a nonlinear MIMO system described in terms of a geometric model of a pin-hole camera with a varying sampling-time. We employ a gain-scheduling approach based on the use of Takagi–Sugeno (T–S) fuzzy models [1], i.e., *fuzzy gain-scheduling* (FGS). The FGS design is a two-step approach (see [2], [3], [4]) – 1) the linearization of the model into a T–S fuzzy model; 2) synthesis of linear controllers and a gain scheduler with guaranteed global stability and robustness properties w.r.t time delays.

In many cases it is very difficult, if not impossible, to obtain the accurate values of time stamp in a system whose control depends on an asynchronous feedback, due to – in the case of our setup– the delays occurring in the feature extraction process. The inaccessibility to the system parameters or on-line variation of the parameters (focal distance or noisy feature reading) are yet another factor for decreased the control performance. This motivates the use of the FGS approach to cope with the parameters' variation aforementioned. The stability analysis of a fuzzy system is not easy, and parameter tuning is generally a time-consuming procedure, due to the nonlinear and multi-parametric nature of the fuzzy control systems. Moreover, it is very important to consider the robust stability against parametric uncertainties in the T–S fuzzy-model-based control systems. This remains to be a central issue in the study of uncertain nonlinear control systems. Robustness in fuzzy model-based control in discrete-time models with fixed sampling-time and parametric uncertainties has been studied before [5]. Asymptotic stability for T–S fuzzy system with fixed and known time-delays was addressed for both the continuous- and discrete-time cases in [6]. Augmented stability with guaranteed-cost design for T–S fuzzy controllers in discrete-time case with fixed sampling-time is presented in [7]. Our novel contribution in this work is to reflect these approaches altogether into a scheme to tackle the problem of uncertainty due to varying sampling-time and unstructured uncertainties. The idea that the system is described as a combination of locally linear sub-models where the varying sampling-time is a premise to the fuzzification motivates the use of FGS approach and performance analysis through LMIs.

The paper is organized as follows: Section II introduces the general scheme for the visual-servoing control problem and presents the camera and image processing model. In section III the model is further developed and discretized into the T-S fuzzy form using the FGS approach. The

Corresponding author[†]: Bourhane Kadmiry, Linköping University, Dept. of Computer and Information Science (AIICS), F490, Grnd floor, Hus-E, SE-581 83 Linköping, Sweden. tel: (+46) 13 284493; fax: (+46) 13 285868. bouka@ida.liu.se

P. Bergsten, Dept. of Technology (AASS), Örebro University. pontus.bergsten@tech.oru.se

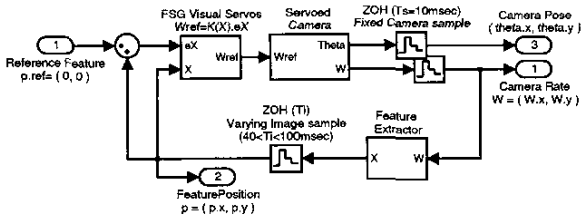

Fig. 1. The visual-servoing scheme

controller design method for robust stabilization in discrete-time of the T–S fuzzy systems in the presence of varying sampling-time and parametric uncertainties is proposed in Section IV. Section V shows controller design feasibility and simulation results. Finally, conclusions are given in Section VI with some discussion.

II. VISUAL-SERVOING SYSTEM

A. General scheme

We will present in this section the global visual-servoing scheme.

The system illustrated by Fig. 1 functions as follows:

- The camera has its own internal rate and pose controllers. Its inputs are reference values of pan/tilt rates ω_x^r and ω_y^r. The output of this subsystem is the camera orientation (pose), θ_x and θ_y, and a video-stream of the region exposed.
- The video-flow is processed by the image-grabber and image-processing subsystem. The image grabber 'samples' the optical flow into separate images (25 images/sec.) which are buffered for further image processing: It is here that time-delays of varying nature occur.
- The image processing inputs the images at a certain rate, and outputs a position $p = [p_x, p_y]$ in image coordinates of a particular feature (see Fig. 1). This data is feeded back in real-time to the visual controller. Furthermore, the position p reading can be altered by noise.
- The objective of the controller subsystem is to position the camera so that the feature is centered in the image (see Fig. 2). It delivers thus a profile of reference values in terms of camera pose-rates to be regulated, to bring the (moving) feature to the center of the image.

Many factors may be responsible for the degraded stability and performance for the control scheme presented above:

- Time-delays can occur from both the feature extraction process or unknown/unmodelled dynamics of the camera control loop: The performance of the feature extraction process could extend from 40 msec. (video-stream rate), to a 100 msec. (computer system interruptions).
- Model parameters and un-modelled dynamics may affect the performance: In our setup, the camera –once mounted on the UAV performing lateral/longitudinal accelerations and turns– will see a degradation of its pan/tilt performance due to Coriolis forces induced by the UAV motion. These conditions affect the performance of the camera, and the dynamics induced are not considered for the control design.

In this work, we will consider these factors as uncertainties in the dynamics of the visual-servoing scheme. The following subsections will present more details about the model used and the measures taken to minimize the action of the factors aforementioned in the performance of the visual-servoing system.

B. Camera and image-processing model

This section is presenting the camera and image-processing (CIP) model. The pan/tilt camera subsystem is basically consisting of two DC motors used for positioning the camera toward a direction of interest. From a system point-of-view, the image processing subsystem is basically consisting of a sampler and a geometric transformation from camera pose/rate to feature position in the image.

In order to derive a model suitable for control design, we make the following assumptions:

1) the CIP subsystems are lumped together and we assume that the resulting system is continuous
2) the control input to the lumped system is angular rate commands $\omega = [\omega_x, \omega_y]$, and the output is the position, $p = [p_x, p_y]$ of the feature in the image frame.
3) the acceleration dynamics of the camera DC-motors are neglected, only the integration part of the dynamics is considered.
4) the model is described w.r.t the camera frame.

The pin-hole camera geometric model is featured as an ideal perspective projection, and represented as follows

$$\begin{bmatrix} p_x \\ p_y \end{bmatrix} = \frac{f}{p_z^c} \begin{bmatrix} p_x^c \\ p_y^c \end{bmatrix} \tag{1}$$

where $p^c = [p_x^c, p_y^c, p_z^c]^T$ is the position of a single feature –represented by the point p^c– in the camera frame centered

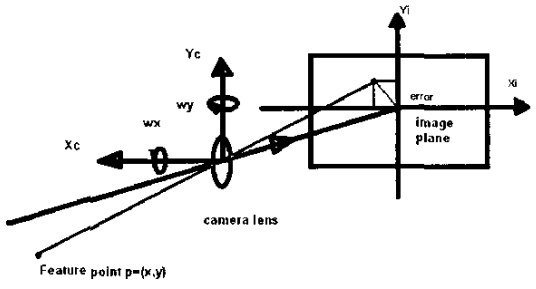

Fig. 2. The control objective

at the pin-hole of the camera. f is the focal distance for the camera lens. Using the assumptions (1-3) above, assuming that the camera moves with translational velocity $\dot{p}^c = [\dot{p}_x^c, \dot{p}_y^c, \dot{p}_z^c]^T$ and angular velocity $\omega = [\omega_x, \omega_y, \omega_z]^T$ and deriving (1) w.r.t time, expressed in the camera frame leads to the optical flow equation

$$\begin{bmatrix}\dot{p}_x\\ \dot{p}_y\end{bmatrix} = \begin{bmatrix} -\frac{f}{p_z^c} & 0 & \frac{p_x}{Z} & \frac{p_x p_y}{f} & -\frac{p_x^2+f^2}{f} & p_y \\ 0 & -\frac{f}{p_z^c} & \frac{p_x}{p_z^c} & \frac{p_y^2+f^2}{f} & -\frac{p_x p_y}{f} & -p_x \end{bmatrix} \begin{bmatrix}\dot{p}^c\\ \omega\end{bmatrix}$$

Using assumption (4) (see also [8]), the camera is constrained only to pan/tilt motions. The CIP model is simplified to the expression

$$\begin{bmatrix}\dot{p}_x\\ \dot{p}_y\end{bmatrix} = \begin{bmatrix} \frac{p_x p_y}{f} & -\frac{p_x^2+f^2}{f} \\ \frac{p_y^2+f^2}{f} & -\frac{p_x p_y}{f} \end{bmatrix} \begin{bmatrix}\omega_x\\ \omega_y\end{bmatrix} \tag{2}$$

where $\dot{p} = [\dot{p}_x, \dot{p}_y]^T$ is the translational velocity of the feature p in the image frame, and $\omega = [\omega_x, \omega_y]^T$ is the angular velocity of the camera. In the standard state-space formulation, the system looks as follows

$$\dot{x} = Ax + B(x)u \tag{3}$$

where $x = [x_1, x_2]^T$ and $u = [u_1, u_2]^T$ denote p and ω, and

$$A = 0_2; \qquad B(x) = \begin{bmatrix} \frac{x_1 x_2}{f} & -\frac{x_1^2+f^2}{f} \\ \frac{x_2^2+f^2}{f} & -\frac{x_1 x_2}{f} \end{bmatrix} \tag{4}$$

The model (3) shows nonlinearities in the B matrix in (4), and has to be furthermore represented in discrete-time. In the following section we will develop further the system using the FGS approach.

III. T-S Fuzzy CIP model design

A. The continuous T-S Fuzzy CIP model

The FGS approach used in this work consists of the following: The original nonlinear model is linearized by bounding the nonlinearities in the state by linear functions [9] – in this way, the nonlinear model is represented by a Takagi-Sugeno fuzzy model, which boils down to convex combination of linear sub-models.

In what follows we will describe in more detail the above design. From (3), we see that there exist three nonlinearities to be dealt with in the control matrix B.

$$b_{11}(x) = -b_{22}(x), \quad b_{21}(x) \quad \text{and} \quad b_{12}(x)$$

These nonlinearities are bounded w.r.t the image size in terms of width and height (x_1, x_2) subject to

$$\begin{aligned} x_1 &\in [-x_{1m}, x_{1m}], \quad x_2 \in [-x_{2m}, x_{2m}] \\ x_{1m} &= 2.210^{-3}m, \quad x_{2m} = 1.910^{-3}m \end{aligned} \tag{5}$$

In order to avoid further confusion between membership functions symbols $b_{nm}(x)$ and their respective boundaries b_{nm}^s, we will use the terms $F_{nm}^s(z)$ for nonlinearities $b_{nm}(x)$, with $z = [x_1, x_2]^T$, $n,m = 1..2$, and $s = i,j,k = 1..2$ relates to the membership regions. For the nonlinear terms in (4) we choose a linear bounding w.r.t (5) such that the fuzzy system obtained represents exactly the nonlinear system in (2). Thus, the membership functions are derived as follows

$$\begin{aligned} F_{11}(z) &= \frac{x_1 x_2}{f} = F_{11}^1 \cdot b_{11}^1 + F_{11}^2 \cdot b_{11}^2; \\ F_{12}(z) &= -\frac{x_1^2+f^2}{f} = F_{12}^1 \cdot b_{12}^1 + F_{12}^2 \cdot b_{12}^2; \\ F_{21}(z) &= \frac{x_2^2+f^2}{f} = F_{21}^1 \cdot b_{21}^1 + F_{21}^2 \cdot b_{21}^2; \\ b_{11}^1 &= -x_{1_m} x_{2_m}; \quad b_{12}^1 = -f - \frac{x_{2_m}^2}{f}; \qquad b_{21}^1 = f; \\ b_{11}^2 &= x_{1_m} x_{2_m}; \quad b_{12}^2 = -f; \qquad b_{21}^2 = f + \frac{x_{2_m}^2}{f} \end{aligned}$$

where $0 \le F_{nm}^1, F_{nm}^2 \le 1$ and $F_{nm}^1 + F_{nm}^2 = 1$. By solving the above equations we obtain the following membership functions:

$$\begin{aligned} F_{11}^1(z) &= \frac{1}{2} - \frac{x_1 x_2}{2x_{1_m} x_{2_m}}; & F_{11}^2(z) &= 1 - F_{11}^1 \\ F_{12}^1(z) &= \frac{x_1^2}{x_{1_m}^2}; & F_{12}^2(z) &= 1 - F_{12}^1 \\ F_{21}^1(z) &= 1 - \frac{x_2^2}{x_{2_m}^2}; & F_{21}^2(z) &= 1 - F_{21}^1 \end{aligned}$$

The graphs illustrating the membership functions F_{nm}^s are shown in Fig. 3. The dynamics of the overall T-S CIP model, is described by a set of 8 fuzzy 'IF–THEN'-rules with fuzzy sets in the antecedents and LTI systems in the consequents. The system in (3) reads now as

$$\dot{x} = \sum_{r=1}^{8} w_r(z)(Ax + B_r u) = \sum_{r=1}^{8} w_r(z) B_r u \tag{6}$$

This system is obtained from a fuzzy rule base where a rule r is of the form

$$r: \text{ IF } z \text{ is } F_{11}^i \text{ and } z \text{ is } F_{12}^j \text{ and } z \text{ is } F_{21}^k \text{ THEN } \dot{x} = B_r u \tag{7}$$

where $w_r(z)$ are weights computed from the membership functions $F_{nm}^s(z)$ for $s = i,j,k = 1..2$ in the IF-part of the rules given a particular value of z,

$$w_r(z) = \frac{F_{11}^i F_{12}^j F_{21}^k}{\sum_{r=1}^{8} w_r(z)} \quad \text{and} \quad \sum_{r=1}^{8} w_r(z) = 1 \tag{8}$$

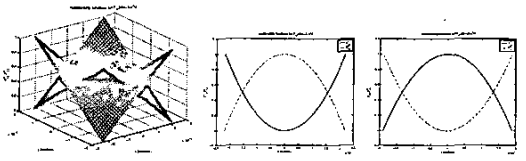

Fig. 3. Membership functions F_{11}^s, F_{12}^s and F_{21}^s

and the control matrix B_r is defined as

$$B_r = B_{ijk} = \begin{bmatrix} b^i_{11} & b^j_{12} \\ b^k_{21} & -b^i_{11} \end{bmatrix}$$

In the following section the model in (6) is discretized. We define furthermore the parameters to consider in the description of the closed-loop for the purpose of the controller design.

B. Discretization of the fuzzy CIP model

The image processing subsystem contains –besides the geometric transformation– an event-based sample-and-hold depending on the unpredictable behavior of the image processing software (IPS). The nominal sample time τ_n is sampling time of the image grabber, which is $\tau_{min} = 40$ msec. However, this sampling-time might increase to $\tau_{max} = 100$ msec. This interval $[\tau_{min}, \tau_{max}]$ represents time-sampling uncertainty. One of the objectives of the control design is to take this varying sample-time in consideration. The discrete-time equivalent to (3) is obtained by using Euler–approximation as follow

$$x_{x+1} = Gx_k + H(x_k)u_k \tag{9}$$

where $x_k = [x_1(k), x_2(k)]^T$, $u_k = [u_1(k), u_2(k)]^T$, $G = I_2$ and $H(x_k) = \tau B(x_k)$. x_{k+1} is the next feature in the image, and τ the sampling time, defined in the interval $[\tau_{min}, \tau_{max}]$. Using the preceding notion, we deduce the discrete-time version of the T–S fuzzy model from (6) and we obtain

$$x_{k+1} = \sum_{r=1}^{8} w_r(z_k)(x_k + \tau_k B_r u_k) \tag{10}$$

with $z_k = [x_1(k), x_2(k)]^T$ and $w_r(z_k)$ are the weights described in section II-B. We consider as well uncertainties contained in the discretized CIP model, described in terms of unstructured norm bounded uncertainties acting on the control matrix H. These uncertainties are assumed to originate from the discretization scheme (Euler–approximation), parameter related uncertainties (focal distance of the camera), as well as noise in the feature position reading. We can not give an explicit quantification of these last two uncertainties, thus we augment (9) and simply write the resulting uncertain system as

$$x_{k+1} = Gx_k + H(x_k)u_k + \Delta H u_k \tag{11}$$

Thus, the equivalent T–S fuzzy model for (11) is as follows

$$x_{k+1} = \sum_{r=1}^{8} w_r(z_k)(x_k + \tau_k B_r u_k + \Delta H u_k) \tag{12}$$

where $\Delta H = \gamma I_2 \Delta I_2$, and Δ is any time-varying matrix such that $\Delta^T \Delta \leq I_2$ and γ is a positive unknown constant describing the *'size'* of the unstructured uncertainty. One other objective of the control design will then be to maximize the closed-loop system robustness w.r.t γ. This will be developed in the next section.

IV. T-S FUZZY CONTROLLER DESIGN

This section presents a fuzzy gain scheduled state-feedback controller for system in (11), which is of the form

$$u_k = -K(z_k)x_k = -\sum_{r=1}^{8} w_r(z_k)K_r x_k \tag{13}$$

where the weights $w_r(z_k)$ are the ones presented in (8). From (11) and (13) we develop the closed-loop as follow

$$x_{k+1} = [I_2 - \tau_k B(x_k)K(z_k) - \Delta H K(z_k)]x_k \tag{14}$$

and the equivalent T–S fuzzy system for (14) develops as

$$x_{k+1} = \sum_{i=1}^{8}\sum_{j=1}^{8} w_i(z_k)w_j(z_k)[I_2 + \tau_k B_i K_j - \Delta H K_j]x_k \tag{15}$$

Notice that, as the control matrix B_i and the control gain matrix K_j differ for each region described by a rule r, ΔH is the same for all the regions. Also, in order to cope with the uncertainty in sampling time, the control matrix H from (11) is represented in the discrete-time version of the rule (7), which is expanded into two rules, as: $H_r = \tau_{min} B_r$ for r_{min} and $H_r = \tau_{max} B_r$ for r_{max}. This increases the number of rules to $r = 16$, and this transformation will –by convexity arguments– guarantee that the system is robust with respect to the varying sampling-time. Each rule r will be expanded as follows

r_{min} : IF z is F^i_{11} and z is F^j_{12} and z is F^k_{21} and τ is τ_{min}
THEN $\dot{x}_k = (I_2 - \tau_{min} B_r K_r - \Delta H K_r)\, x_k$

r_{max} : IF z is F^i_{11} and z is F^j_{12} and z is F^k_{21} and τ is τ_{max}
THEN $\dot{x}_k = (I_2 - \tau_{max} B_r K_r - \Delta H K_r)\, x_k$

Notice that, in both the rules r_{min} and r_{max}, the gain K_r is the same. The objective of the control design is to compute the feedback gains $K_j, (j = 1..8)$, so that

- the closed loop H_2 performance is guaranteed for the system as described in (10) , that is, without unstructured uncertainties ΔH.
- the system in (12) is robustly stable with as big γ as possible to cope with the uncertainties.

This is a multi-objective controller design problem w.r.t the above mentioned objectives. The following subsections describe how to design the controller for the two objectives separately.

A. Optimal H_2 cost design

The discrete-time performance for a fixed and known time-delay controller of a has been discussed in [6]. Optimal H_2 cost for discrete-time T–S without delays is presented in [7]. In this section, we combine these results for the discrete-time version with varying sampling-time as described by (10). We show that the problem of minimizing an upper bound on a quadratic performance measure can be recast as a trace minimization problem. This is done subject to a set of LMIs, which guarantees that the quadratic cost of the system would not exceed a specified limit. To achieve

guaranteed H_2 performance, the following cost function is minimized

$$J = \sum_{j=1}^{\infty} x_k^T Q x_k + u_k^T R u_k \tag{16}$$

subject to (10) and (13). This is the common LQR cost-function used in linear optimal control (see [7]). Minimizing the cost function (16) results in finding the positive-definite matrix P, solution of the following Lyapunov equation

$$(G-HK)^T P(G-HK) - P + Q + K^T R K = 0;$$
$$K = R^{-1} H^T P$$

where $Q \geq 0$ and $R \geq 0$ and $Y = P^{-1}$. For easing the annotations we define the matrices N_{ik} and O_{ijk} as follows

$$\begin{aligned} N_{ik} &= G_i Y - \tau_k B_i K_i Y; \\ O_{ijk} &= (G_i + G_j) Y - (\tau_k B_i K_j + \tau_k B_j K_i) Y \end{aligned} \tag{17}$$

The solution of the optimal cost problem is dealt using the LMI approach by solving the following optimization problem

Min tr(Z) Subject to

$i = 1..8, j < i \leq 8, k = 1..2$

$$\begin{bmatrix} Z & I_2 \\ I_2 & Y \end{bmatrix} > 0; \ (a)$$

$$\begin{bmatrix} Y & N_{ik}^T & YQ^{\frac{1}{2}} & X_1^T R^{\frac{1}{2}} & \dots & X_8^T R^{\frac{1}{2}} \\ N_{ik} & Y & 0 & 0 & \dots & 0 \\ Q^{\frac{1}{2}} Y & 0 & I_2 & 0 & \dots & 0 \\ R^{\frac{1}{2}} X_1 & 0 & 0 & I_2 & \dots & 0 \\ \vdots & \vdots & \vdots & \vdots & \ddots & \vdots \\ R^{\frac{1}{2}} X_8 & 0 & 0 & 0 & \dots & I_2 \end{bmatrix} > 0; \ (b)$$

$$\begin{bmatrix} Y & O_{ijk}^T & YQ^{\frac{1}{2}} & X_1^T R^{\frac{1}{2}} & \dots & X_8^T R^{\frac{1}{2}} \\ O_{ijk} & Y & 0 & 0 & \dots & 0 \\ Q^{\frac{1}{2}} Y & 0 & I_2 & 0 & \dots & 0 \\ R^{\frac{1}{2}} X_1 & 0 & 0 & I_2 & \dots & 0 \\ \vdots & \vdots & \vdots & \vdots & \ddots & \vdots \\ R^{\frac{1}{2}} X_8 & 0 & 0 & 0 & \dots & I_2 \end{bmatrix} > 0 \ (c)$$

(18)

In order to cope with the uncertainty in sampling time, the LMI constraints that contain the control matrix H are duplicated into two LMIs: one with $H_r = \tau_{min} B_r$ and the other with $H_r = \tau_{max} B_r$ as we did for the rules in section IV. If the above LMIs are feasible, we calculate the controller gains as

$$K_i = X_i Y^{-1} \tag{19}$$

The obtained K_i's make the closed-loop asymptotically stable w.r.t the varying τ.

B. Optimal robust stability design

Robust fuzzy control for a system as described by (12) is treated in [5]. Using this framework for our problem, we obtain the optimally robust fuzzy controller w.r.t unstructured uncertainties in (15) by solving the following LMI optimization problem

Min α Subject to

$i = 1..8, j < i \leq 8, k = 1..2$

$$\begin{bmatrix} -Y & N_{ik}^T & YK_i^T & 0 & 0 \\ N_{ik} & -Y & 0 & I_2 & I_2 \\ K_i Y & 0 & -I_2 & 0 & 0 \\ 0 & I_2 & 0 & -\alpha I_2 & 0 \\ 0 & I_2 & 0 & 0 & -\alpha I_2 \end{bmatrix} < 0; \ (a)$$

$$\begin{bmatrix} -4Y & O_{ijk}^T & -YK_j^T & -YK_i^T & 0 & 0 \\ O_{ijk} & -Y & 0 & 0 & I_2 & I_2 \\ K_j Y & 0 & -I_2 & 0 & 0 & 0 \\ K_i Y & 0 & 0 & -I_2 & 0 & 0 \\ 0 & I_2 & 0 & 0 & -\alpha I_2 & 0 \\ 0 & I_2 & 0 & 0 & 0 & -\alpha I_2 \end{bmatrix} < 0 \ (b)$$

(20)

where $\alpha = \sqrt{\frac{1}{\gamma^2}}$. The matrices N_{ik} and O_{ijk} are defined in (17). In order to cope with the uncertainty in sampling time, we use the same strategy as described in subsection IV-A, doubling the number of LMIs related to the 8 rules for τ_{min} and τ_{max}. If the above LMIs are feasible, we calculate the controller gains as described in (19), and the obtained K_i's make the closed-loop robust w.r.t the varying τ.In the following subsection we consider a combined optimal control problem.

C. Combined cost and robust stability controller design

The multi-objective robust optimal controller problem is solved by minimizing a combined objective function subject to the combination of both the LMIs constraints in sections IV-B and IV-A as follows

$$\begin{aligned} &\textbf{Min } \lambda\alpha + (1-\lambda) tr(Z) \quad \textbf{Subject to} \\ &\quad i = 1:..8, j < i \leq 8 \\ &\text{LMI (18) - (a) and (b),} \quad \textit{and} \\ &\text{LMI (20) - (a) and (b)} \end{aligned} \tag{21}$$

If the above LMIs are feasible, we can calculate the controller gains as described in (19). Once the controller gains are found, the global T-S controller can be obtained using (13).

V. Simulation and Experiments

In this section, we will illustrate an application of the proposed controller, and perform a number of numerical simulations. We will next, show results issued from a real camera platform.

Using results from section IV-C, for the given model parameters in terms of image size and focal distance, we perform the design with the following H_2 cost parameters

Q and R in (18), and the weighting parameter λ in (21). These parameters are set to: $Q = Diag(10^{-4}, 10^{-4}), R = Diag(10^{-6}, 10^{-6})$, and $\lambda = .001$. We achieve feasibility of the problem in (21), and by minimizing the linear objective, we obtain the P matrix verifying the optimal robustness augmented by a guaranteed cost

$$P = \begin{bmatrix} 3.0334 & 0 \\ 0 & 3.0339 \end{bmatrix} 10^6$$

We achieve a feasible solution of required accuracy with

- best objective value: J = $6.22\ 10^6$
- $tr(Z) = 6.07\ 10^6, \gamma = 79\ 10^{-6}$

Next, we will perform a series of simulations in *Matlab – Simulink*. These simulations are executed comparing the behavior of the system with regards to time-sample variations, for each control channel (pan and tilt). The controllers are implemented in C-language and are used to control the real camera platform as well.

The first simulation is performed for the regulation of position reference values of a point p (image feature), for both sampling times $\tau_{min} = 40$ msec. and $\tau_{max} = 100$ msec. All values of sampling-time within the limits $[\tau_{min}, \tau_{max}]$ show stable behavior. Fig. 4 shows the response by regulation w.r.t $p^d = (0,0)$.

Fig. 4 shows both the error profiles (upper-part) and the camera regulation responses for the x-channel (middle-part) and y-channel (lower-part). The regulation is done for the size of the image. The error is settled to zero after ≈270 msec. for the system sampled at $\tau = 40$ msec., while for the system sampled at $\tau = 100$ msec., the error settles after ≈230 msec. The middle- and lower-parts of Fig. 4 show a step-response for each channel. The system sampled at τ_{min} has a smoother response, which translates to a camera rotation without *shake*, which in term translates to a settlement without overshoot. The system sampled at τ_{max} has a dead-beat behavior with faster response (up to

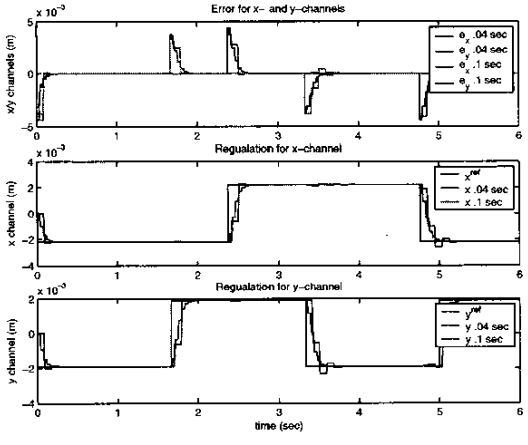

Fig. 4. Comparison between systems sampled at 40 and 100 msec. for regulation

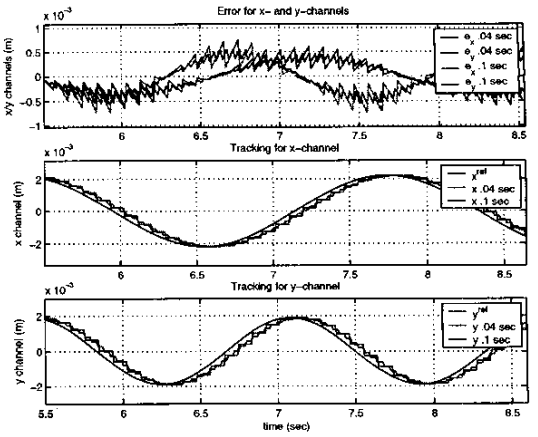

Fig. 5. Comparison between systems sampled at 40 and 100 msec. for tracking

140 msec. to reach 90% of the reference value) and an overshoot of (≈ 6%).

The second simulation is performed for the tracking of the same feature, for both sampling times $\tau_{min} = 40$ msec. and $\tau_{max} = 100$ msec. with inducing in the reference values an error profile of a sinusoidal shape. Fig. 5 shows both the error profiles (upper-part) and the camera tracking responses for x-channel (middle-part) and y-channel (lower-part). The tracking error presents a saw-teeth shaped oscillation around the sinusoidal shape of the error fluctuation. This oscillation is due to the integration factor that the sampled position undergo in the closed-loop, thus is more pronounced for the time sampling τ_{max}. The oscillation does not appear in the regulation case because of the signal flatness between two reference values. The oscillation is bounded to ≈ 8% of the error amplitude, while the error fluctuation is bounded to ≈ 2% of the amplitude of the tracked profile of reference. The delays between reference values and output response for the tracking scheme are respectively about 80 msec. for the system sampled at $\tau = 40$ msec. and 70 msec. for the one at $\tau = 100$ msec., that is for both the channels (x,y).

Third, we run an experiment on the real camera platform, for regulation. Fig. 6 show a scenario in which a beacon whose pattern permits to identify the feature is placed suddenly in the image field of a the camera. The camera is controlled in angular rate control mode, and responds by centering the feature in the image.Fig. 6 shows both the error profiles (upper-part) and the camera pose responses for the x-channel (middle-part) and y-channel (lower-part). The last two profiles in Fig. 6 are in degrees, and these readings are done at sampling time of ≈88 msec. The x-channel presents an overshoot of ≈ 14%, with a time response of ≈ 1.3 sec. for both channels.The profiles show overshoots for both the x- and y-channels; this occurs mainly due to coupling between the two channels. The time responses for the real platform are longer than this of simulation model.

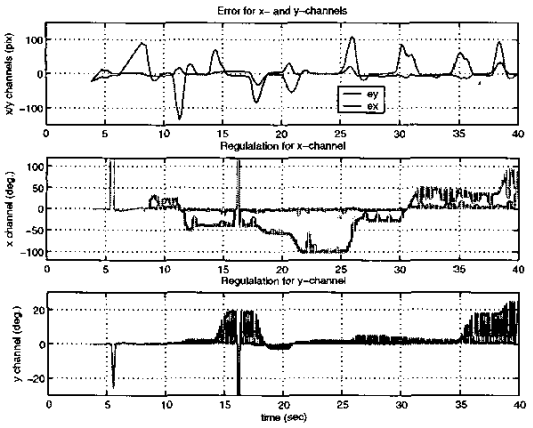

Fig. 6. Camera angles regulation using angular rate control

This is due to the camera DC-motor closed-loop dynamics, which are not taken into account in the model used for simulation.

Last, we proceed similarly as experiment 3, with moving the camera over the pattern, or moving the pattern in front of the camera. This results in a profile tracking scheme whose results are illustrated in Fig. 7. Both the error profiles for the x- and y-channels are shown in the upper-part of Fig. 7, and the camera pose responses for the x-channel (middle-part) and y-channel (lower-part) illustrate the rotation of the camera in pan and tilt in order to center the feature in the image. The amplitude of the error fluctuation is higher the one in the simulation case. This is due to the latency of the camera DC-motors responses to the control signal. The last two profiles in Fig. 7 are in degrees. The sudden artifacts in the pose profiles are mainly due to reading errors of the camera angles (absence of sensor-data when queried by the control software), and do not affect in any case the control

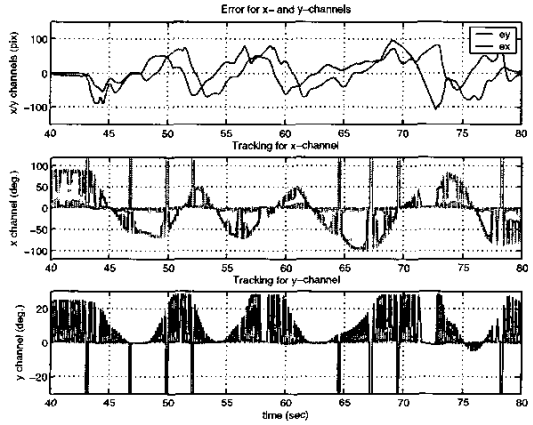

Fig. 7. Camera angles tracking using angular rate control

performance.

VI. Conclusions

This paper presented a novel method for the design of a fuzzy gain scheduled visual-servoing controller for a pan/tilt camera whose characteristics and dynamics are partially known and whose control-loop depends on image processing of a tracked feature which suffers a varying sampling-time. The controller is based on a nonlinear geometric model. This setup was tested in both extensive simulation and experiments on the real camera platform, The results show the effectiveness of the proposed design method.

The next step in this work will be dedicated to exploring the robustness of the system developed to both sampling-time uncertainty and external disturbances in actual UAV flight senarii.

VII. Acknowledgments

The authors would like to thank Pr. D. Driankov of the Dept. of Technology (AASS), Örebro University, for his helpful suggestions and guidance. We would as well like to express our gratitude to the Knut and Alice Wallenberg Foundation in Sweden whose financial support made this work possible.

References

[1] T. Takagi and M. Sugeno, *Fuzzy identification of Systems and its Applications to Modeling and Control*, In: IEEE Trans. Systems, Man and Cybernetics, SMC-15(1), pp. 116–132, Jan. 1985.

[2] D. Driankov, R. Palm and U. Rehfuss, *A Takagi-Sugeno fuzzy gain scheduler*, In: IEEE Conference Fuzzy Systems Proceedings, New Orleans, Florida, USA, 1996, pp. 1053–1059.

[3] P. Korba, *A gain-schedulling approach to model-based fuzzy control*, Fortschritt-Berichte VDI num.837, IBSN 3-18-383708-0, VDI Verlag GmbH, Dusseldorf, 2000.

[4] P. Bergsten, M. Persson and B. Iliev, *Fuzzy gain scheduling for flight control*, In: IEEE Conference on Industrial Electronics, Control and Instrumentation Proceedings, Nagoya, Japan, 2000.

[5] H.J. Lee, J.B. Park, G. Chen, *Robust fuzzy control of nonlinear systems with parametric uncertainties*, In : IEEE trans. on Fuzzy Systems, Vol-9, num. 2, Apr. 2001.

[6] H.O.Wang, K.Tanaka, *Fuzzy Control System Design and Analysis: a LMI approach* , a Wiley-Interscience Publication, John Wiley and Sons, Inc. New York, NY. 10158-0012.

[7] A. Jadbabaie, et al., *Guaranteed-cost design of Takagi-Sugeno fuzzy controllers via LMIs*, In : IEEE International Conference on Fuzzy Systems, Anchorage, AK, USA, 1998.

[8] M. Sznaier, O. I. Camps, *Control issues in active-vision: Open problems and some answers*, In: 37th IEEEConference on Decisionand Control Proceedings, Tampa, Florida, USA, 1998.

[9] K. Tanaka et al., *Generalized Takagi-Sugeno Fuzzy Systems: Rule Reduction and Robust Control*, In: 9th IEEE Int. Conf. on Fuzzy Systems, 2: pp. 688–693, San Antonio, TX-USA, May 2000.